

Determination of Richardson number profile from remote sensing data and its aviation application

P W Chan

Hong Kong Observatory, 134A Nathan Road, Kowloon, Hong Kong, China

E-mail: pwchan@hko.gov.hk

Abstract. A number of remote-sensing wind-measuring instruments, such as LIDAR and radar wind profilers, have been set up in the vicinity of the Hong Kong International Airport (HKIA) for monitoring of low-level windshear and turbulence. The combined usage of wind data from a radar wind profiler and boundary layer temperature profiles from a ground-based microwave radiometer in turbulence application is studied in this paper. Data collected in a field experiment of the radiometer conducted in Hong Kong in February 2006 were used to obtain the Richardson number profile up to 1.5 km above ground. Two examples of atmospheric turbulence reported by the pilots are considered. The Richardson number profiles are found to capture the turbulence events reasonably well. The evolution of these profiles and airflow disruption by the nearby terrain as a possible cause of the turbulence will also be discussed.

1. Introduction

The Hong Kong International Airport (HKIA) is situated in an area of complex terrain (Figure 1). To its south is the mountainous Lantau Island with peaks rising to about 1000 m above mean sea level with valleys as low as 400 m in between. When winds from the east to southwest climb over Lantau Island, turbulent airflow may occur in the vicinity of the airport. Turbulence could have significant impact on aviation safety. A dense network of anemometers is operated by the Hong Kong Observatory (HKO) to monitor the turbulence condition in the airport area [1]. Studies have also been conducted on the use of measurements from radar wind profilers [1], Doppler Light Detection And Ranging (LIDAR) systems [2] and Terminal Doppler Weather Radar (TDWR) [3] to monitor turbulence. The locations of these instruments are shown in Figure 1.

The above monitoring methods are based on the fluctuations of the wind field as revealed in the spectrum width or the structure function of the radial velocity provided by the remote-sensing, wind-measuring equipment. Richardson number [4] is another useful parameter for turbulence monitoring and it combines both the thermodynamic and the dynamic profiles in the troposphere. Whilst the wind profiles are measured basically continuously by radar wind profilers in Hong Kong, temperature profiles are only available twice a day from radiosonde.

In 2006, a field experiment was conducted in Hong Kong on the study of aviation applications of a ground-based, multi-channel microwave radiometer [5]. The radiometer gave temperature profiles up to 10 km in the atmosphere nearly continuously. This paper examines the combination of wind profiles from radar wind profilers with the temperature profiles from the radiometer during the field experiment in the calculation of Richardson number and discusses its potential application in the monitoring of turbulence to be encountered by the aircraft.

Section 2 describes the instruments used in this study. Calculation of Richardson number from the instrumental data is discussed in Section 3. Two case studies of the application of Richardson number profiles are then presented, one for a departure runway in Section 4, and another for an arrival runway in Section 5. Conclusions of the paper are drawn in Section 6.

2. Instruments

The vertical wind profiles in this study are provided by the two radar wind profilers near HKIA, namely, Siu Ho Wan and Sha Lo Wan profilers (locations in Figure 1). They belong to boundary-layer type and operate at a frequency of 1299 MHz. The Siu Ho Wan profiler measures in both the low and high modes: the low mode starts at 116 m above ground, with a height increment of 60 m up to about 1500 m; the high mode starts at 260 m above ground, with a height increment of 200 m up to about 6000 m. The Sha Lo Wan profiler operates in the low mode only. Wind profiles are available every 10 minutes. They are obtained by processing the spectrum data from the wind profilers using NCAR Improved Moments Algorithm (NIMA) [6].

The microwave radiometer uses 7 frequencies in the oxygen channel to measure the vertical profile of the temperature. It works in two modes, viz. elevation mode for boundary-layer scanning and zenith mode for measuring in the whole troposphere. The present paper only uses the data of the former mode. It gives temperature data every 50-100 m in the first 1000 m above ground and every 150 – 200 m between 1000 and 2000 m. Temperature profiles were updated every 16 minutes or so during the field experiment in 2006, and more frequent update is possible by changing the scan strategy. The radiometer was located at Siu Ho Wan (Figure 1) during the experiment. Since there was only one radiometer in the study, its data will be used in this study of turbulence both to the east and to the west of HKIA.

3. Calculation of Richardson number

As discussed in [5], the Richardson number Ri is defined as:

$$Ri = \frac{\frac{g}{\theta} \frac{\partial \theta}{\partial z}}{\left[\left(\frac{\partial U}{\partial z} \right)^2 + \left(\frac{\partial V}{\partial z} \right)^2 \right]} \quad (1)$$

where g is the acceleration due to gravity, θ the potential temperature, U the east-west component of the wind, V the north-south component of the wind, and z the height. The atmospheric condition is favourable for the occurrence of turbulence when $Ri <$ the critical Richardson number $Rc = 0.25$.

The vertical gradients of wind components are readily calculated from the wind measurements of the low-mode and the high-mode (when available) of the radar wind profiler (in order to get to the height of the pilot turbulence report). To minimize the effect of rapid fluctuations of the wind components on the vertical gradient, the wind profiles have been processed by binomial smoothing for two times. Similar smoothing has also been carried out in the study of Scorer parameter profile for mountain waves [7].

The potential temperature profile and its gradient are computed from the temperature data of the radiometer. Since pressure data above ground are not available, the pressure measurement at the surface and the upper-air temperature data are used to calculate the upper-air pressure values by hydrostatic approximation. Because the temperature profile from the radiometer is generally rather smooth, no further smoothing is applied to the temperature data in the calculation of vertical gradient.

4. Case 1 – 26 February 2006, over a departure runway

Two aircraft departing to the east from the north runway of HKIA, viz. over 07LD runway corridor (Figure 1) reported light to moderate turbulence between 2500 feet (about 760 m) and 5000 feet (about 1500 m) at 20:56 and 21:13 UTC, 26 February 2006. The Richardson number profiles at the closest times of wind and temperature measurements to these two events, namely, 20:39 and 21:09 UTC on that day are evaluated. To examine the evolution of the atmospheric conditions for this case, the profiles at 3-4 hours before and after the events are also considered, namely, at 17:11 UTC, 26 February and 01:03 UTC, 27 February. In this study, Ri profiles separated by several hours are considered in order to see the evolution of the chance of occurrence of turbulent airflow due to changes of the mesoscale circulation and the thermodynamic structure.

The potential temperature profiles at the above four times are shown in Figure 2(a). The atmosphere between 500 and 2000 m is generally stable at all times with the potential temperature increasing with height. Among the four times, the profile at 21:09 UTC is slightly more stable between 600 and 1200 m or so with a larger vertical gradient of potential temperature.

The vertical profiles of U and V (without smoothing) are given in Figures 2(b) and (c) respectively. For U component, the profiles at the times of the turbulence events have larger gradient between 600 and 1100 m in comparison to the other two profiles. For V component, the vertical gradients at 20:39 UTC, 26 February between 1000 and 1500 m, and that at 21:09 UTC, 26 February between 900 and 1200 m, are larger than the other two times. Though the wind is generally from the southeast in the lower boundary layer and veers to westerly at about 2000 m for all the four times under consideration, the vertical gradients of the wind components do not stay more or less constant, but show variation with time.

The larger wind component gradients result in the occurrence of Ri less than the critical value of 0.25 for some altitudes during the turbulent airflow events over 07LD runway corridor. The Richardson number profiles at the above four times are shown in Figure 2(d). At 20:39 UTC, Ri is less than the critical value between 700 and 1300 m. The corresponding altitude range at 21:09 UTC is between 800 and 1100 m over which the wind gradient offsets the slightly more stable boundary layer leading to generally smaller absolute values of Ri among the four times. These results are largely consistent with the reported heights of turbulent airflow by the pilots. The Ri values at 17:11 UTC, 26 February and 01:03 UTC, 27 February are generally larger than 0.25 over these altitudes.

It is also noted that, at the above four times, the Ri could be less than 0.25 below 400 m or so, especially the occurrence of negative Ri value. This feature is mainly related to turbulent airflow associated with thermodynamic instability near the ground. However, there were no pilot reports of turbulence at such altitudes closer to the ground.

The appearance of turbulence in the airport area is also examined using the LIDAR data. The conical scan at 4.5-degree elevation angle from the horizon by the first LIDAR (location in Figure 1) is shown in Figure 2(e), depicting the prevalence of southeasterly flow of ~17 m/s within the boundary layer. Unfortunately, the LIDARs and the TDWR did not good signals at the locations of the reported turbulence in this case (at about 4 nautical miles, or 8 km or so, away from the eastern end of the north runway of HKIA). The best available wind data at the event locations come from the Tung Chung Gap vertical-slice scan of the first LIDAR (scan location in Figure 1). The radial velocity data from this scan at 20:41 UTC, 26 February is shown in Figure 2(f). The blockage of the laser beam at about 500 m above mean sea level over Lantau Island in this scan appears to be due to clouds associated with the airflow climbing over the gap from the southeast. Downstream of this airflow, there are a number of waves/vortices between 700 and 1600 m high with the dimensions of several hundred metres in height and a couple of kilometres in the horizontal. Following the argument similar to that in [8], if such features exist downstream of the gap to the west of Sunset Peak – Lin Fa Shan (locations in Figure 1), they may be expected downstream of the gap to the east of these hills as well, which is just near the locations of the turbulence reports. The physical mechanism for turbulence in the present case would require further studies. A possible reason is the shear instability associated with quick veering of the wind with height.

5. Case 2 – 27 February 2006, over an arrival runway

Two aircraft landing at the north runway of HKIA from the west, viz. over 07LA runway corridor (Figure 1), reported moderate turbulence at 11:21 and 11:34 UTC, 27 February 2006 at a height of 800 feet (about 240 m) and 1300 feet (about 390 m) respectively. The Richardson number profile at the wind and temperature measurements closest to these events, namely, 11:20 UTC, 27 February, is considered. Similar to the previous Section, the profiles at 3-4 hours before and after the events, namely, 08:10 and 15:10 UTC, 27 February, are also examined.

The potential temperature profiles at the above three times are shown in Figure 3(a). The gradient of potential temperature between 250 and 400 m at 11:20 UTC is slightly smaller than the other two times over the same range of altitude.

The vertical profiles of U and V (without smoothing) are shown in Figures 3(b) and (c) respectively. With smoothing (not shown), the U profiles at the three times have very small vertical gradients only between 250 and 400 m. The gradients of the smoothed V profiles have larger values for 08:10 and 11:20 UTC over this range of altitude, whereas the corresponding value at 15:10 UTC remains rather small.

Figure 3(d) gives the Richardson number profiles at the three times. The Ri at 11:20 UTC below ~600 m is less than 0.25, thus favouring the occurrence of turbulent flow. This is largely consistent with the pilot turbulence reports. Both dynamic and thermodynamic instability could play a role in this case because Ri could be positive and negative below ~600 m. On the other hand, the Ri values in this range of altitudes at 08:10 and 15:10 UTC are generally larger than 0.25. At the three times, the general veering of the wind with height is the same, namely, the east to southeasterly flow near the surface veers to southerly flow at about 1500 m above mean sea level. However, there are differences in the gradients of the wind components as well as the potential temperature, leading to rather different behaviour of Ri values.

TDWR image of radial velocity in the conical scan of 0.6-degree elevation angle from the horizon at 11:21 UTC, 26 February is given in Figure 3(e). For an aircraft landing at 07LA runway, it would first encounter the mountain wake (decelerated flow downstream of the hills on Lantau Island) and then the east to southeasterly jet within the first couple of nautical miles from the runway end. The mountain wake area and the interface between the wake and the jet have rather turbulent flow, as shown by the spectrum width data of TDWR (Figure 3(f)). The spectrum width could get as large as 5.5 – 6.5 m/s. The relationship between TDWR's spectrum width and the cube root of eddy dissipation rate (EDR), the internationally adopted metric of turbulence for aviation application, has not yet been established, but based on correlation equations established in limited case study results [4], the above range of spectrum width value corresponds to $EDR^{1/3}$ much larger than $0.3 \text{ m}^{2/3} \text{ s}^{-1}$, i.e. moderate turbulence or above. The EDR profiles obtained by the glide path scans of the first LIDAR (not shown) following the method in [3] also have maximum values of about $0.28 \text{ m}^{2/3} \text{ s}^{-1}$. Both TDWR and LIDAR measurements support the occurrence of turbulent airflow over 07LA runway corridor.

6. Conclusions

The aviation application of Richardson number profile calculated from remote sensing data, namely, monitoring of turbulence encountered by the aircraft, is discussed in this paper through two examples. The profile is determined from wind data from radar wind profilers as well as temperature data from a ground-based microwave radiometer. The continuous availability of the measurements from these instruments enables the frequent update of the profile. Besides the Richardson number profiles near the times of the turbulence reports, those at 3-4 hours before and after the events are also considered to examine the evolution of the atmosphere in the mesoscale. It turns out that, while the general veering of the wind with height remains about the same over many hours, the vertical gradients of the wind components could be quite different, leading to different behaviour of the Ri values. The changes in the vertical gradient of potential temperature also contribute to the evolution of Richardson number

profile. In general, the height ranges over which Ri less than the critical value of 0.25 are generally consistent with the turbulence reports from the pilots.

The present paper only considers the Richardson number profile over a limited period of time due to the short-term availability of the microwave radiometer in the field experiment in 2006. HKO has recently installed a permanent unit of radiometer at HKIA. With this installation, more data will become available to study the operational application of Richardson number profile in the monitoring of turbulence.

References

- [1] Chan PW and Chan ST 2004: Performance of eddy dissipation rate estimates from wind profilers in turbulence detection. *11th Conference on Aviation, Range, and Aerospace Meteorology*, American Meteorological Society, Hyannis, MA, USA, 4-8 October 2004
- [2] Kwong KM and Chan PW 2007: LIDAR-based turbulence intensity calculation along glide paths. *14th Coherent Laser Radar Conference*, Snowmass, Colorado, USA, 8-13 July 2007
- [3] Chan PW, Li CM and Wong KH 2007: Use of spectrum width data from the Terminal Doppler Weather Radar (TDWR) for monitoring turbulence intensity: case studies. *First Asian Conference on Radar in Meteorology and Hydrology*, Hubei, China, 22-24 October 2007
- [4] Stull RB 1988: *An Introduction to Boundary Layer Meteorology*, Kluwer Academic Publishers, 670 pp.
- [5] Chan PW, Wu KC and Shun CM 2006: Applications of a ground-based microwave radiometer in aviation weather forecasting. *13th International Symposium for the Advancement of Boundary Layer Remote Sensing*, Garmisch-Partenkirchen, Germany, 18-20 July 2006
- [6] Morse CS, Goodrich RK and Cornman LB 2002: The NIMA method for improved moment estimation from Doppler spectra. *J. Atmos. Oceanic Technol.*, **19**, 274–295.
- [7] Chan PW 2007: Atmospheric waves associated with a valley of Lantau Island: observation, theory and numerical simulation. *12th Conference on Mesoscale Processes*, American Meteorological Society, Waterville Valley, New Hampshire, USA, 6-9 August 2007
- [8] Banta RM and co-authors, 2006: *Detection and diagnosis of wind shear and turbulence using Doppler LIDAR at Hong Kong International Airport*. ESRL/NOAA and HKO, 130 pp.

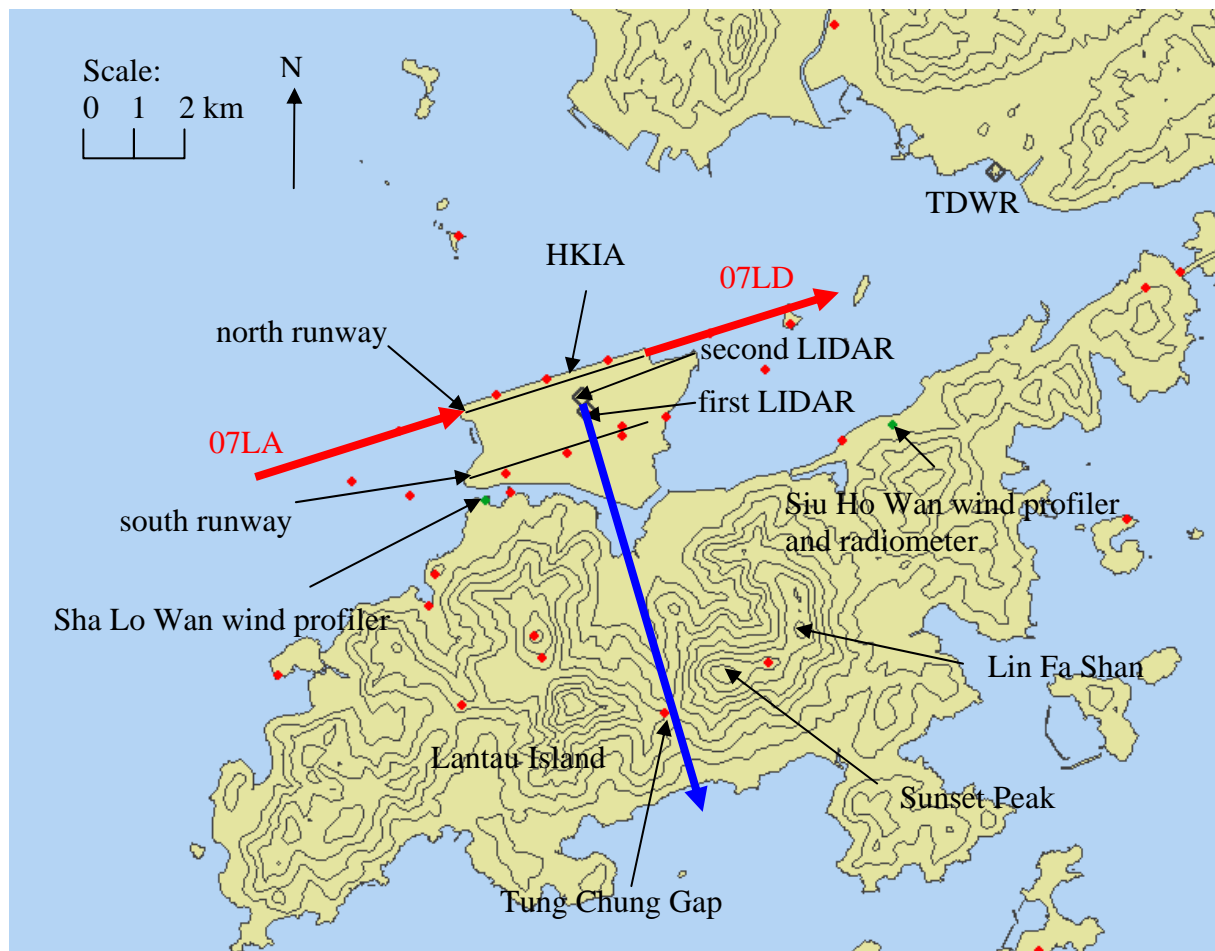


Figure 1. Geographical situation near HKIA. Height contours are in 100 m. Locations of the meteorological instruments considered in this paper are indicated. Red dots are the surface anemometers and weather buoys. The two runway corridors of HKIA discussed in the main text are depicted by red arrows, showing the directions of aircraft movements. Blue arrow is the direction of Tung Chung Gap vertical slice scan of the first LIDAR.

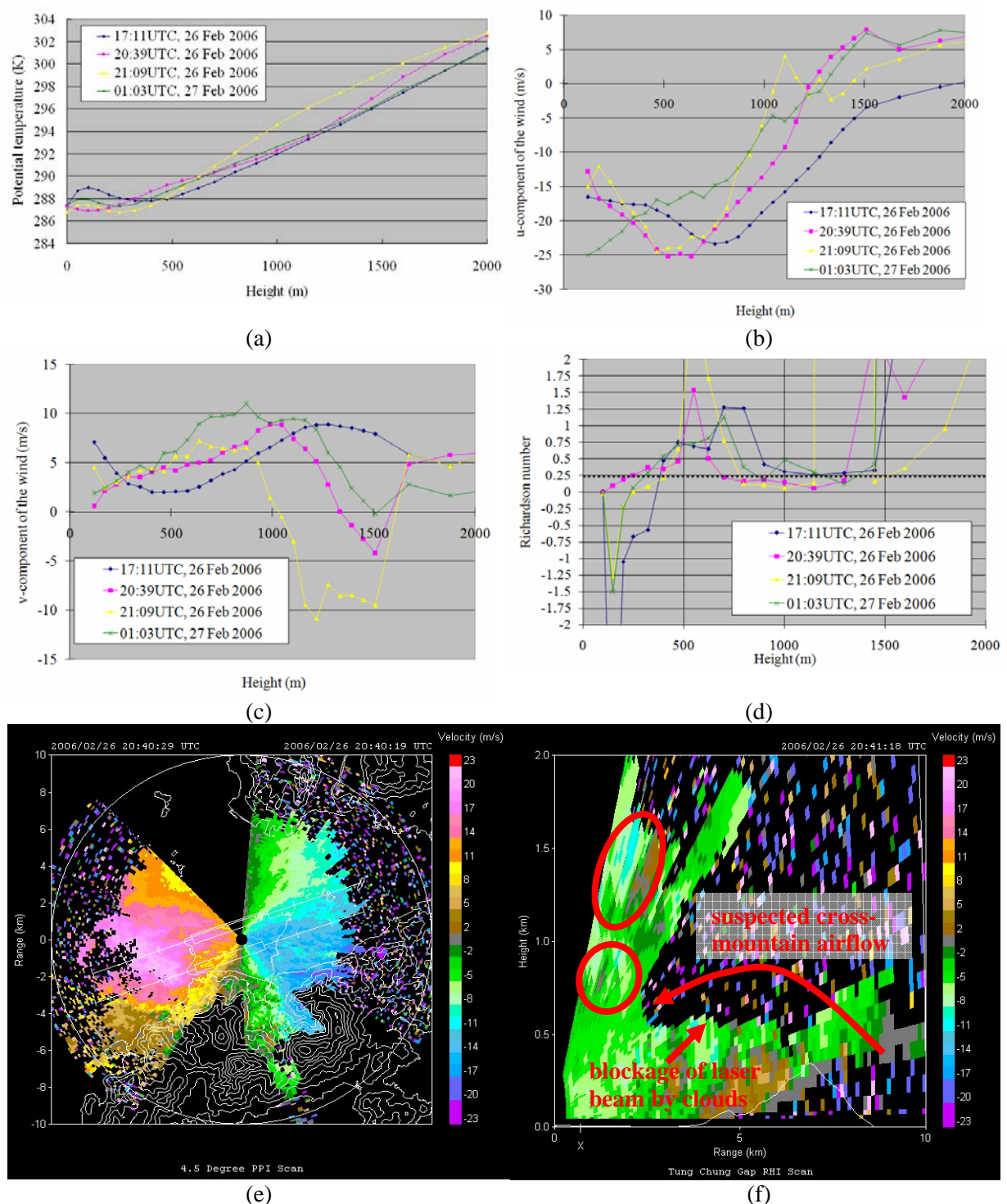


Figure 2. For the case study on 26 February 2006: (a) potential temperature profiles, (b) profiles of east-west (U) component of the wind, (c) profiles of north-south (V) component of the wind, (d) Richardson number profiles, (e) 4.5-degree conical scan of radial velocity by the first LIDAR, with the velocity scale on the right hand side; the white “skeletons” from the runways are the extended centrelines with tick marks at every nautical mile up to 3 nautical miles away, and (f) Tung Chung Gap vertical slice scan of the first LIDAR, with the velocity scale on the right hand side; the waves/vortices

discussed in the main text are enclosed in red ellipses.

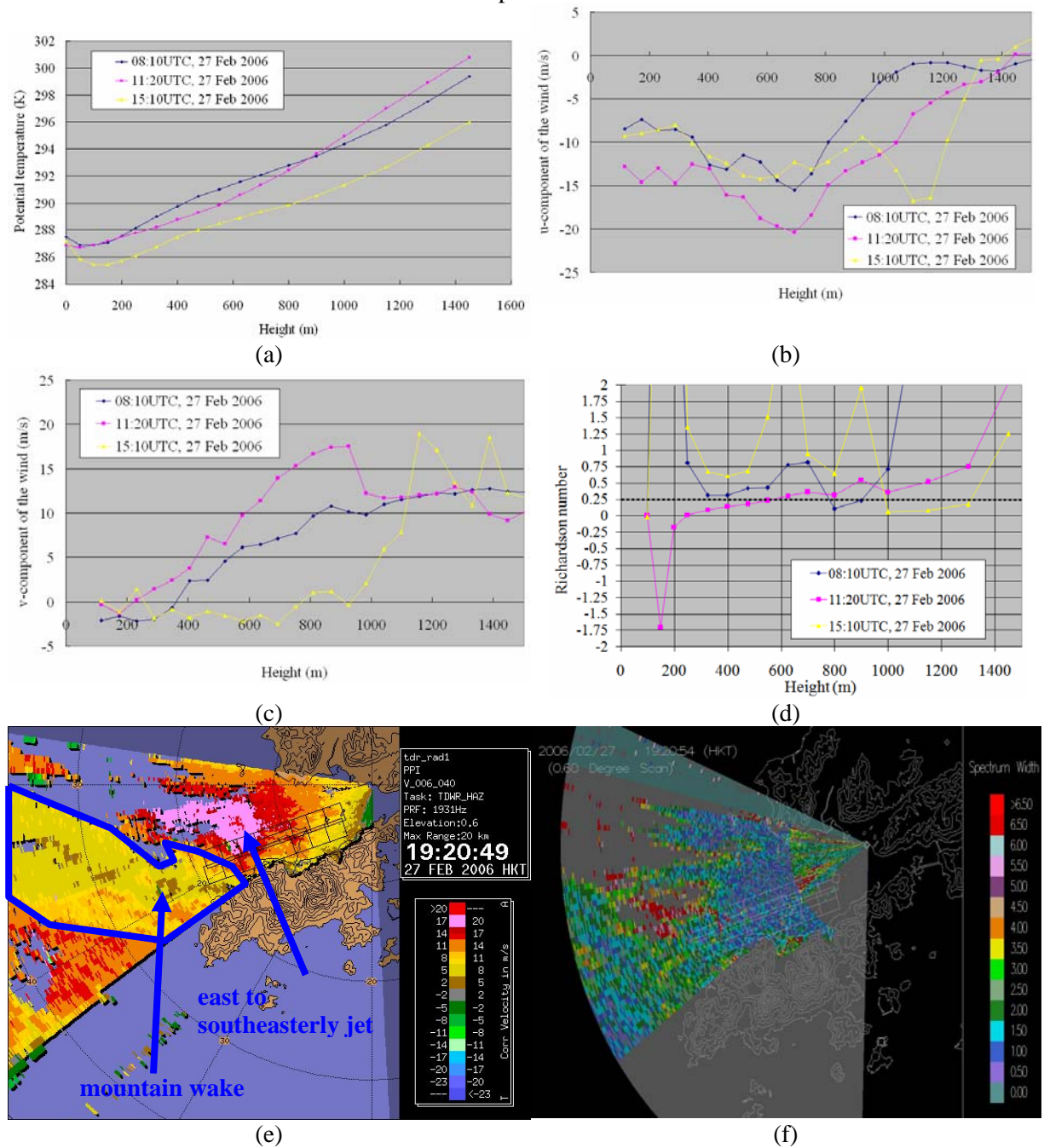


Figure 3. For the case study on 27 February 2006: (a) to (d) same as those in Figure 2, (e) TDWR image of radial velocity at the surveillance scan of 0.6-degree elevation angle from the horizon, (f) the spectrum width image of TDWR at the time corresponding to (e).